RSC Advances

ROYAL SOCIETY OF CHEMISTRY

www.rsc.org/advances

ARTICLE TYPE www. rsc.org/xxxxxx | XXXXXXXX

Electron transport properties of fulgide-based photochromic switches

G. A. Nemnes[*a,b] **and Camelia Visan**[b]

Received Xth XXXXXXXXXX 20XX, Accepted Xth XXXXXXXXX 20XX
First published on the web Xth XXXXXXXXXX 200X
DOI: 10.1039/b000000x

The transport properties of fulgide-based photochromic switches are investigated in the framework of density functional theory calculations. In our setup light activated furyl-fulgide molecules are coupled to nanoscopic metallic electrodes. The electrocyclization process under UV light converts the open-ring into a closed-ring conformation. Conversely, the reverse process takes place by visible light illumination. The switching properties are firs analyzed in linear bias regime revealing a high conductance ratio between the open and closed configurations The robustness of the results is investigated by analyzing comparatively two compounds from the same family, namely furyl- and thiophene fulgides. For both systems, at finit applied bias, one can establish three working regimes, which correspond in turn to a photochromic switch, a negative differential conductance element or to a logical inverter, pointing out the versatility of the considered fulgide based devices.

1 Introduction

The ongoing scaling of electronic devices for memory and logic applications, beyond the physical limits of standard semiconductor technology, has brought into attention the importance of molecular switches[1–5]. For this purpose molecules with bistable states are required, generated by magnetic spin states or by changing their geometric configura tions, which may be driven by heat, light, pressure[6,7]. The photochromic molecular switches are one particular example recently investigated, both experimentally and theoretically, of promising candidates for three-dimensional optical storage technology.

A well known class of photochromic molecules represented by diarylethenes[8] has been already investigated for potential electronic applications[9–14]. Besides diarylethenes, one can mention other examples of optical switches based on dihydroazulene[15], dihydropyrene[16], spiropyran[17], or spirooxazine[18]. The molecules are attached to metallic electrodes or carbon nanotubes. Upon irradiation with visible and UV light, the molecules can be reversibly switched between two different conformations introducing a measurable change in the electrical response. One usually assigns the ON- and OFF states to the high- and low conductivity states, respectively. The ratio of the on-off currents is considered a measure of performance for this type of switching devices.

We investigate here another class of photochromic molecules, namely the fulgides[19,20], which posses similar desirable properties as e.g. diarylethenes: thermal irreversibility, a rather good photostability and relatively high spectral separation of the closed and open ring isomers. Charge transfer has been analyzed in finit molecular systems, of type donor-switch-acceptor[21], e.g. anthracene acting as donor and coumarin moiety as acceptor, by means of fs transient-absorption spectroscopy[22]. A recent study presents the ring-opening photochemistry of fulgide molecules and derivatives, as promising candidates for energy modulation devices, nonlinear optical materials or photobiological applications like controlling the enzyme or protein conformations[20]. The macroscopic properties have been investigated to a large extent and a wide range of applications has been proposed, such as multi-level recording[23], optical storage of information using circular dichroism in a chiral nematic phase[24] etc. Furthermore, the effects of conformational transformations on electronic transport properties of fulgimides – amide derivatives of fulgides, sandwitched between gold bulk electrodes have been investigated[25].

In this paper we focus on the characterization of the conduction properties of an optical switch with fulgide molecules as active elements. Photocyclization reactions induce an isomer change, from closed- to open ring conformation. This processes typically take only a few hundreds femtoseconds as revealed by femtosecond time-resolved spectroscopy[26] and time-dependent density functional theory (DFT) calculations on single molecules. In our setup nanoscopic metallic electrodes for contacting the molecules are considered. The chemical binding between the electrodes and fulgide molecule in

[a] *University of Bucharest, Faculty of Physics, Materials and Devices for Electronics and Optoelectronics Research Center, P.O. Box MG-11, 077125 Magurele-Ilfov, Romania. Fax: +40 (0)21 457 4418; Tel: +40 (0)21 457 4949/157; E-mail: nemnes@solid.fizica.unibuc.ro.*
[b] *Horia Hulubei National Institute for Physics and Nuclear Engineering (IFIN-HH), 077126 Magurele-Ilfov, Romania.*

different conformations is described in the framework of DFT. Next, the transmission functions are calculated using nonequilibrium Greens functions formalism. We investigate the ratio between the currents obtained for the two conf gurations, open and closed, in order to establish the possibility of using fulgide molecules for electro-optical switches. Furthermore, two types of fulgides, furyl- and thiophene fulgide, are investigated comparatively in order to analyze the feasibility of the approach. In addition, the nonlinear bias regime reveals the existence of three distinct working regimes suitable for different sub-nanometer electronic components.

2 Model and Method

The device model is depicted in Fig. 1 illustrating the active element, the photochromic 3-furyl fulgide, 2-[1-(2,5-dimethyl-3-furyl)-ethylidene]-3-isopropylidene succinic anhydride, contacted by aluminum nanoscopic electrodes. The furyl fulgide molecule presents three stable isomers[19] labeled by *C*, *E* and *Z*. The *C*-isomer, representing the closed conformation, is colored and mostly planar having an extended π-electron system, which is the source of the large absorption in the visible region. The *E*-isomer, representing the open conformation, is colorless with absorption in the UV region. In this case, the furyl-ring is rotated around the fulgide-ring which suppresses the π-conjugated system. The *Z*-isomer is also an open conformation isomer, a conformer of the *E*-isomer and therefore with a similar absorption spectrum. However, since the molecule is attached to the Al electrodes by the carbon atoms connected to the fulgide ring, the relevant photocycling reaction paths for this set-up are given by the $C \rightarrow E$ and $E \rightarrow C$ switching.

The structural optimizations are performed in the framework of DFT calculations, implemented by SIESTA[27], which uses a set of numerical atomic orbitals as basis set – a prerequisite for linear scaling of the computational time with the system size. In our calculations we used a double-zeta polarized (DZP) basis set, with the orbital-conf ning cutoff radii specif ed by an energy shift of 0.02 Ry and the standard split norm for the generation of multiple zeta in the split valence scheme of 0.15. Norm-conserving Troullier-Martins pseudopotentials were used. The local density approximation (LDA) is used in the parametrization proposed by Alder[28]. The sampling of the Brillouin zone is performed using a Monkhorst-Pack scheme with $1 \times 1 \times 8$ *k*-points. A mesh cut-off of 200 Ry was used and all the structures were relaxed until the residual forces were less than 0.04 eV/Å. Both fulgide conformations, open and closed, as well as the nanoscopic Al electrodes are initially relaxed separately and subsequently the system is assembled and the geometry of the whole structure is once again optimized.

Next, the ballistic transmission is calculated by non-equilibrium Green's functions (NEGF) technique. We analyze both linear and non-linear bias regimes, pointing out the differences which appear in conduction by switching from the closed to the open conformation. In the calculation of the current we employ the Landauer formula:

$$I = \frac{2e}{h} \int dE \; \mathscr{T}(E;U) \; [f_{\mathrm{FD}}(E;\mu_{\mathrm{L}}) - f_{\mathrm{FD}}(E;\mu_{\mathrm{R}})], \quad (1)$$

where the transmission function is calculated from

$$\mathscr{T}(E;U) = \mathrm{Tr}[\Gamma_{\mathrm{L}}(E;U) G^{r}(E;U) \Gamma_{\mathrm{R}}(E;U) G^{a}(E;U)]. \quad (2)$$

In the NEGF technique the transmission function is determined using the advanced/retarded Green's functions $G^{a/r}$ and the self-energies $\Gamma_{\mathrm{L/R}}$ describing the coupling between the molecular system and the contacts. The chemical potentials in the left and right contacts are $\mu_{\mathrm{L}} = eU/2$ and $\mu_{\mathrm{R}} = -eU/2$, set by the applied bias U. In the linear bias regime ($\mu_{\mathrm{L}} \simeq \mu_{\mathrm{R}} = \mu$) and in limit of low temperatures we may write the conductance as $G = 2e^2/h \; \mathscr{T}(\mu;U \rightarrow 0)$.

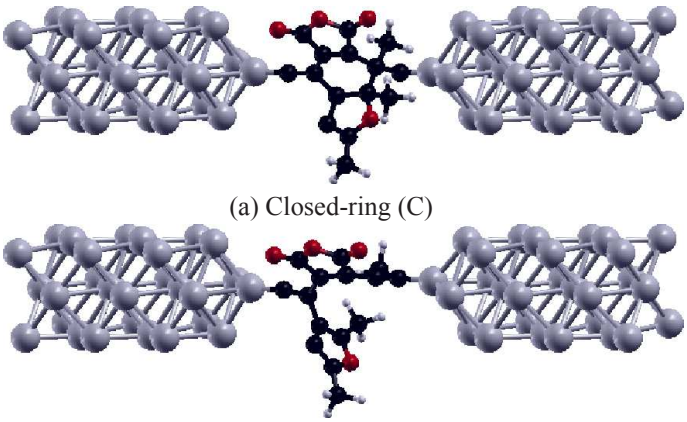

(a) Closed-ring (C)

(b) Open-ring (E)

Fig. 1 Device structure with the fulgide molecule in the closed (a) and open (b) ring conformations.

3 Results and discussion

3.1 Structural properties

We f rst examine the structural properties of the nanoscopic electrodes, which consist of A-B type stacking along the [001] direction of fcc-Al. Due to the small cross-section, the structural parameters deviate from the bulk values, as it was reported in similar thin columnar electrodes[5] and in other undercoordinated systems such as atomic clusters. Aluminum electrodes have been used in the context of molecular electronic devices[29–31], atomic-sized contrictions being produced by break-junction techniques[32], while recently Al contacts

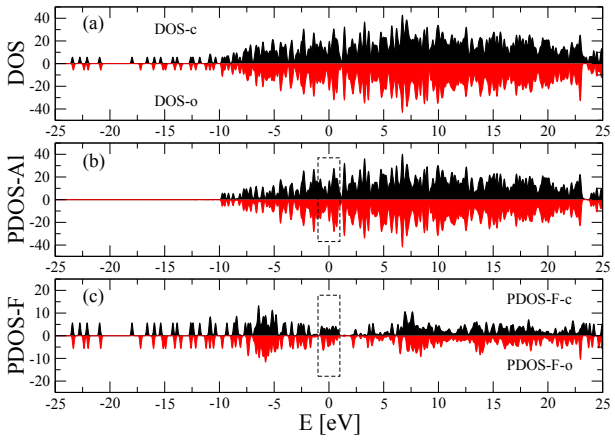

Fig. 2 Total and partial density of states: (a) Total density of states for the furyl fulgide molecule and Al contacts, in the closed (DOS-c) and open (DOS-o) configuration (mirrored); (b) PDOS-Al, totalizing states in the Al contacts; (c) PDOS-F-o and PDOS-F-c, corresponding to the fulgide molecule, for the open and closed configurations respectively. The rectangles mark the relevant energy window around the chemical potential ($\mu = 0$).

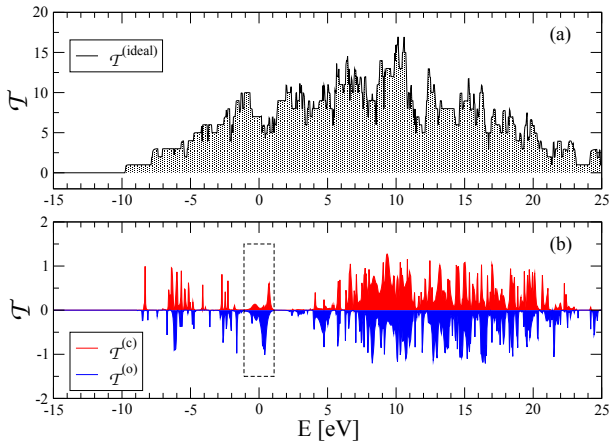

Fig. 3 Transmission functions for the pristine Al nanowire (a) and for the furyl fulgide system connected to electrodes (b), for both closed and open conformations (mirrored). The energy window around the chemical potential is marked by dashed line.

were used in graphene fiel effect transistors[33]. In addition there is a renewed interest in the structure and conductance of aluminum nanocontacts[34]. The Al electrodes have potential advantages over the standard gold counterparts, such as e.g. atomic scale oxidation can provide thin barriers, largely localized s-p valence orbitals, as opposed to transition metals, which allows direct bonding to organic molecules and efficien charge injection into the linker and a rather flat gapless density of states even in the case of thin nanoscopic contacts. In our setup the electrodes are generated by a 9-atom unit cell, with 5 atoms in the layer A and 4 atoms in the layer B. The optimized structural parameters are $a_A = 3.9$Å and $a_B = 4.2$Å, whereas the value for the bulk lattice constant of fcc-Al is $a_0 = 4.05$Å. Consequently, A-type layer is slightly contracted, while the B-type layer is slightly expanded compared to the bulk value. The distance between A- and B-type layers is contracted to $d_{AB} = 3.8$Å. The semi-infinit electrodes are placed at fi ed positions, with the distance between the tips $\Delta = 10$Å, corresponding to the initial state without fulgide molecule attached.

Following optimizations of isolated fulgide isomers, a careful analysis of the coupling between them and the Al nanocontacts is performed. The C-Al bonding is a central topic in organoaluminium chemistry[35,36], which is one of the major themes within organometallic chemistry. The tips of the electrodes are connected to the carbon atoms on the opposite sides of the hexagonal ring. It is worth mentioning that in experimental setups spacer chains are often used, e.g. ethinyl groups, to reduce the possibility of a shortcircuit between electrodes, at the same time providing an enhanced control over the anchoring points. In addition, the spacer chains may prevent a strong interaction between the electrodes and other atoms of the fulgide molecule, while the electrode tips are kept at a proper distance. The fulgide molecule is placed between the two Al electrodes and structural optimizations are performed for the entire system. In the relaxed configuratio the distance between the tips of the electrodes is reduced by pulling forces exerted by the molecule to 9.6Å and 9.8Å for the *C* and *E* isomers, respectively. The (average) C-Al bonding length obtained is 1.88Å with small deviations, depending on the contact and isomer. The distance between the tip of the electrode and the neighboring Al atoms is increased which is one indication of the strength of the C-Al bonds. Furthermore, the analysis of the total energies shows the difference between the open and closed conformations of the isolated fulgide molecule is 0.62 eV, while for the molecular systems with electrodes attached one obtains an energy difference of 0.48 eV, indicating the switching is still accessible.

3.2 Linear bias regime. PDOS analysis.

The transport properties of the molecular system are firs investigated in the linear bias regime. To a large extent, the charge transfer characteristics can be explained by the total and partial density of states, which are indicated in Fig. 2. The total density of states is found by summing up the partial densities of states (PDOS) corresponding to the electrodes (PDOS-Al) and fulgide molecule (PDOS-F). The metallic contacts exhibit a rather continuous spectrum, while isolated groups of peaks are visible for the fulgide molecule.

We analyze the transmission functions of the pristine Al

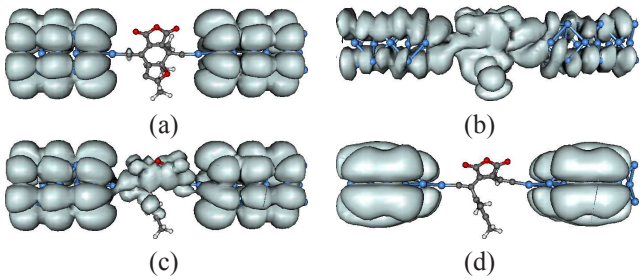

Fig. 4 Molecular orbitals (absolute value square) for the closed (a,b) and open (c,d) conformations at two different energies, $E = 0.4$ eV (a,c) and $E = 0.6$ eV (b,d). The two states correspond to the prominent peaks in Fig. 3(b) in the energy window around the chemical potential.

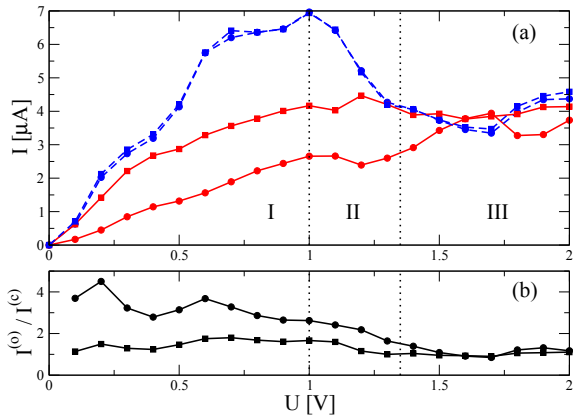

Fig. 5 Nonlinear bias regime. (a) The current vs. bias is depicted for furyl fulgide (circles) and thiophene fulgide (squares), for the closed (red/solid) and the open (black/dashed) conformations (mirrored). (b) The on-off current ratio, $I^{(o)}/I^{(c)}$, of the open and closed conformations vs. bias, for furyl fulgide (circles) and thiophene fulgide (squares).

nanowire and for the molecular system in both open and closed conformations. A step-wise transmission function is obtained for the ideal Al wire, shown in Fig. 3(a), which indicates the number of propagating modes at each energy. Despite the small cross-section the Al wire exhibits good conduction properties, which can be correlated with the gapless spectrum plotted in Fig. 2(b). The molecule filter out some energies and the resulting transmission function is a series of peaks, with the positions closely correlated with the PDOS-F presented in Fig. 2(c). More specificall , the transmission functions $\mathscr{T}^{(o/c)}$ ploted in Fig. 3(b) are given to a high extent by the overlap between the PDOS-Al and PDOS-F. In the linear regime the ON-OFF ratio is given by ratio of the conductances in the two configurations $G^{(o)}/G^{(c)} = 3.3$, with the transmission functions evaluated at the chemical potential. Although by comparison the on-off ratio of diarylethenes is about two orders of magnitude [12], one may still distinguish between the two working regimes of the proposed fulgide-based device.

The transmission peaks in the vecinity of the Fermi energy are correlated with the molecular orbitals depicted for two values of the energy, for the closed and open conformations in Fig. 4. At $E = 0.4$ eV the transmission is significantl larger in the open conformation compared to the closed one. At $E = 0.6$ eV the opposite is found.

3.3 Non-linear bias regime. Furyl- and thiophene fulgides.

We investigate the robustness of the switching properties by analyzing the finit bias regime. In addition, we also compare the transfer characteristics of the furyl fulgide molecule with another compound from the fulgide family, namely the thiophene fulgide. As the molecules are quite similar, the optimized structures differ mostly by an increased C-S bonding length of $\sim$1.78Å compared to the length of the C-O bond $\sim$1.41Å. The I-V characteristics are plotted in Fig. 5(a). In the open configuration the furyl fulgide and thiophene fulgide show very similar results. This is supported by the fact the main contribution to the transport is ensured by the atomic carbon chain, with a lesser influenc exerted by the thienyl moiety. By contrast, in the closed configuration the two compounds exhibit rather different I-V dependence. An overall smaller current is obtained for the furyl fulgide, which enhances the switching ratio $I^{(o)}/I^{(c)}$, as compared with the thiophene fulgide. In this case, due to the higher electronegativy of oxygen in furan compared to sulfur in thiophene, the oxygen atom attracts its electrons more strongly, leading to a larger delocalization in thiophene and consequently the conductance is enhanced compared to the furyl fulgide system.

We can further distinguish three regimes, which correspond to different bias intervals. The firs one, define by $U < 1$V, shows a close to ohmic regime for both compounds in either open or closed conformations. Observing the trend in Fig. 5(b) the on-off ratio is declining with the increase of the applied bias. However, besides the switching functionality, two other working regimes are established at higher biases. In the second region, define by $1 < U < 1.35$V, the transfer characteristics of the open conformations exhibit negative differential conductance. This behavior can be inferred from bias dependent transmission functions ploted in Fig. 6. At low voltages there is a steady increase of the current as the energy window is getting larger and the transmission function is varrying slowly. Beyond 1V, in the case of the open conformation, the transmission function drops continously at energies around the Fermi level, while the prominent peak is further shifted at the edge of the energy window, which causes a decrease of the

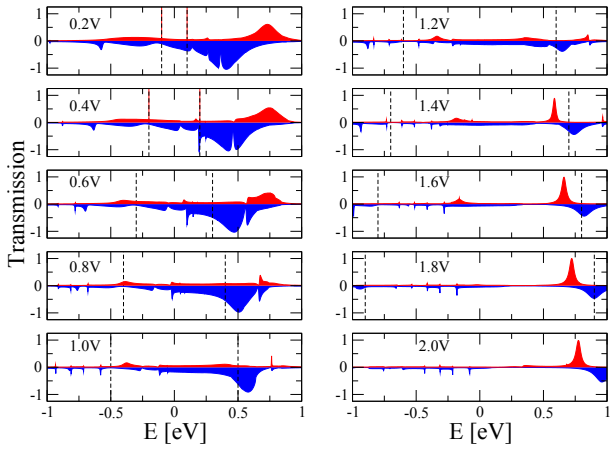

Fig. 6 Transmission functions in the non-linear bias regime for closed (red) and open (blue) conformations. The vertical dashed lines mark the energy window at each bias.

total current. Beyond 1.35V, a third regime may be pointed out: the I-V characteristics of closed and open conformations are crossing and, consequently, the ON-state is turned into the OFF-state and vice versa. This ensures the functionality of a logical inverter. To fully assess this feature, the relaxation of the structures in the large voltage range is necessary. This features are observed in the considered setup with aluminum nanoscopic electrodes. Both types of molecules exhibit this behavior, however a larger amplitude for the furyl fulgide system is obtained.

Increasing the functionality within the same space is one goal of modern electronics. Reconfigurabl devices allow distinct functionalities to be integrated in the same circuit. Compared to the other photochromic switches which have been previously investigated, the fulgide family shows an enhanced versatility, i.e. one obtains three different functionalities in the same device.

4 Conclusions

Molecular photochromic switches based on fulgides were investigated in the framework of density functional theory calculations. Using the non-equilibrium Green's functions technique, the transport properties were analyzed for the closed and the open ring conformations. The results obtained for the linear bias regime show there is a clear difference in conduction properties of the two conformers. This trend is also recovered in the nonlinear bias regime, confirmin the robustness of the approach. Next, we analyzed comparatively furyl fulgides and thiophene fulgides molecules. Both compounds indicate a similar behavior in the switching properties, with a higher on-off current ratio in the case of furyl fulgides. Furthermore, the I-V characteristics in the nonlinear regime presents three working regimes: (I) a quasi-ohmic regime, with a clear distinction between the closed- and open conformation in the I-V characteristics – suitable for an optical switch, (II) a negative differential conductance regime for the closed ring configura tion and (III) an inverter operating regime, all of them controlled by the applied bias. In summary, fulgide molecules can serve as next generation photochromic switches, but at the same time they prove to be versatile active elements for reconfigurabl nanometer-sized electronics.

References

1 B. Y. Choi, S. J. Kahng, S. Kim, H. Kim, H. W. Kim, Y. J. Song, J. Ihm and Y. Kuk, *Phys. Rev. Lett.*, 2006, **96**, 156106.
2 J. Henzl, M. Mehlhorna, H. Gawronski, K. H. Rieder and K. Morgenstern, *Angew. Chem., Int. Ed.*, 2006, **45**, 603.
3 J. M. Seminario, P. A. Derosa and J. L. Bastos, *J. Am. Chem. Soc.*, 2002, **124**, 10266.
4 G. K. Ramachandran, T. J. Hopson, A. M. Rawlett, L. A. Nagahara, A. Primak and S. M. Lindsay, *Science*, 2003, **300**, 1413.
5 G. A. Nemnes and A. Nicolaev, *Phys. Chem. Chem. Phys.*, 2014, **16**, 18478.
6 P. Gütlich, A. Hauser and H. Spiering, *Angew. Chem., Int. Ed. Engl.*, 1994, **33**, 2024.
7 S. J. van der Molen, J. H. Liao, T. Kudernac, J. S. Agustsson, L. Bernard, M. Calame, B. J. van Wees, B. L. Feringa and C. Schonenberger, *Nano Lett.*, 2009, **9**, 76.
8 P. Zhao, P. Wang, Z. Zhang, C. Fang, Y. Wang, Y. Zhai and D. Liu, *Solid State Commun.*, 2009, **149**, 928.
9 Y. Kim, T. J. Hellmuth, D. Sysoiev, F. Pauly, T. Pietsch, J. Wolf, A. Erbe, T. Huhn, U. Groth, U. E. Steiner and E. Scheer, *Nano Lett.*, 2012, **12**, 3736.
10 D. Kim, H. Jeong, H. Lee, W.-T. Hwang, J. Wolf, E. Scheer, T. Huhn, H. Jeong and T. Lee, *Adv. Mater.*, 2014, **26**, 3968.
11 B. M. Briechle, Y. Kim, P. Ehrenreich, A. Erbe, D. Sysoiev, T. Huhn, U. Groth and E. Scheer, *Beilstein J. Nanotechnol.*, 2012, **3**, 798.
12 A. Staykov, D. Nozaki and K. Yoshizawa, *J. Phys. Chem. C*, 2007, **111**, 3517.
13 L. Zhu, K. A. Yao and Z. L. Liu, *Appl. Phys. Lett.*, 2010, **97**, 202101.
14 K. Matsuda, *Pure Appl. Chem.*, 2008, **3**, 555.
15 C. J. Xia, D. S. Liu and H. C. Liu, *Sci. China Mech. Astron.*, 2011, **54**, 437.
16 P. Zhao, C.-F. Fang, Y.-M. Wang, Y.-X. Zhai and D.-S. Liu, *Curr. Appl. Phys.*, 2009, **9**, 1213.
17 E. Malic, A. Setaro, P. Blummel, C. F. Sanz-Navarro, P. Ordejon, S. Reich and A. Knorr, *J. Phys.: Condens. Matter.*, 2012, **24**, 394006.
18 H. Zhao, Y. Xua, W. Zhao, K. Gao and D. Liu, *Physica B*, 2014, **437**, 41.
19 Y. Yoshioka, M. Usamib, M. Watanabe and K. Yamaguchi, *J. Mol. Struct.*, 2003, **623**, 167.
20 B. C. Arruda and R. J. Sension, *Phys. Chem. Chem. Phys.*, 2014, **16**, 4439.
21 I. Ramsteiner, A. Hartschuh and H. Port, *Chem. Phys. Lett.*, 2001, **343**, 83.
22 A. Hartschuh, I. Ramsteiner, H. Port, J. Endtner and F. Effenberger, *J. Lumin.*, 2004, **108**, 1.
23 Y. Chen, T. Li, M. Fan, X. Mai, H. Zhao and D. Xu, *Mater. Sci. Eng. B*, 2005, **123**, 53.
24 M. L. Bossi, J. B. Rodriguez and P. F. Aramend, *J. Photochem. Photobiol. A: Chem.*, 2006, **179**, 35.
25 Y. yuan He and J. wei Zhao, *J. Electrochem.*, 2014, **20**, 243.

26 R. Siewertsen, F. Renth, F. Temps and F. Sönnichsen, *Phys. Chem. Chem. Phys.*, 2009, **11**, 5952.

27 J. Soler, E. Artacho, J. Gale, A. Garcia, J. Junquera, P. Ordejon and D. Sanchez-Portal, *J. Phys.: Condens. Matter*, 2002, **14**, 2745.

28 D. Ceperley and B. Alder, *Phys. Rev. Lett.*, 1980, **45**, 566.

29 C. Morari, I. Rungger, A. R. Rocha, S. Sanvito, S. Melinte and G.-M. Rignanese, *ACS Nano*, 2009, **3**, 4137.

30 B. Larade, J. Taylor, H. Mehrez and H. Guo, *Phys. Rev. B*, 2001, **64**, 075420.

31 S. Wohlthat, F. Pauly, J. K. Viljas, J. C. Cuevas and G. Schön, *Phys. Rev. B*, 2007, **76**, 075413.

32 E. Scheer, J. C. C. N. Agra, A. L. Yeyati, B. Ludoph, A. Martin-Rodero, G. R. Bollinger, J. M. van Ruitenbeek and C. Urbina, *Nature*, 1998, **394**, 154.

33 J. Zheng, L. Wang, R. Quhe, Q. Liu, H. Li, D. Yu, W.-N. Mei, J. Shi, Z. Gao and J. Lu, *Sci. Rep.*, 2013, **3**, 1314.

34 T. Ohko and T. Kizuka, *J. Nanosci. Nanotechnol.*, 2015, **15**, 5180.

35 M. Witt and H. W. Roesky, *Curr. Sci.*, 2000, **78**, 410.

36 S. Alnemrat and J. P. Hooper, *J. Chem. Phys.*, 2014, **141**, 144304.